Supporting Information

Lanthanide-Organic Gels (LOGs) as a Multifunctional Supramolecular Smart Platform

José Yago Rodrigues Silva[a], Leonis Lourenço[b] da Luz, Filipe Gabriel Martinez Mauricio[c], Iane Bezerra Vasconcelos Alves[a], Jamylle Nunes de Souza Ferro[d], Emiliano Barreto[d], Ingrid Távora Weber[a,c], Walter Mendes de Azevedo[a,b], and Severino Alves Júnior [a,b]*

AUTHOR INFORMATION

[a] Materials Science Program, Federal University of Pernambuco (UFPE), 50670-901, Recife, PE, Brazil

[b] Fundamental Department of Chemistry, Federal University of Pernambuco (DQF-UFPE), 50670-901, Recife, PE, Brazil. Tel. +55 81 2126-7475; Fax: +55 81 2126-8442; e-mail:salvesjr@ufpe.br.

[c] Inorganic and Materials Laboratory, University of Brasília (LIMA-UnB), 70910-000, Asa Norte, Brasília, DF, Brazil. Tel. +55 61 3107 3898

[d] Laboratory of Cell Biology, Federal University of Alagoas, 57072-970, Maceió, AL, Brazil

Corresponding Author

* Prof. Dr. Severino Alves Júnior, Fundamental Department of Chemistry, UFPE, 50670-901, Recife, PE, Brazil. Tel. +55 81 2126-7475; Fax: +55 81 2126-8442; E-mail: salvesjr@ufpe.br

Experimental Section

Synthesis of G-Ln: The G-Ln (Ln = Nd, Sm, Eu, Gd, Tb, Dy, Ho, Er, Tm, Yb and Lu) hydrogels were synthesized based on a previously reported method.[1] In brief, the synthesis was improved in two steps. In the first step, 0.45 mmol of iminodiacetic acid (H_2IDA) and 0.075 mmol of Ln_2O_3 was added to a glass reactor containing 4 mL of aqueous solution. Then, the solution was irradiated by microwaves under heavy stirring at 160ºC (100 W) for10 min. In the second step, the solution pH was adjusted to 9 using a basic solution (NaOH, 1 M) and further gelation was trigged by re-irradiation under microwaves at 160ºC (100 W) for 10 min.

Synthesis of G-mix: Mixed-metal hydrogels were obtained using the above mentioned method and changing the lanthanide stoichiometry, leading to a total of 27 mixed hydrogel sample types: G-$Eu_{1-x}Tb_x$ (x= 0.10, 0.25, 0.50 and 0.75), G-$Gd_{0.9}Eu_{0.1-x}Tb_x$ (x= 0.025, 0.050 and 0.075), G-$Gd_{0.8}$ $Eu_{0.2-x}Tb_x$ (x= 0.05, 0.10 and 0.15), G-$Gd_{0.7}Eu_{0.3-x}Tb_x$ (x= 0.10, 0.15 and 0.20) and G-$Gd_{0.4}Eu_{0.6-x}Tb_x$ (x= 0.2, 0.3 and 0.4).

Theoretical calculations: Optimization and SCF calculations were performed in terms of DFT/B3LYP/6-31G approximation built in GAMESS software package.[2] The spatial distribution of the HOMO and LUMO was obtained using Avogadro software.[3]

Cell viability assay: Were used the fibroblast NIH/3T3 cell line to evaluate the cytotoxic effect. For this, MTT assay was carried out in 96-wells plate. A volume of 200 µl of 2×10^5 cells mL^{-1} were maintained for 24 h in CO_2 chamber, in DMEM-Advanced supplemented with 10% fetal bovine serum (FBS), 1% L-glutamine and 40 µg mL^{-1} gentamycin. The biocompatibility of the hydrogels (G-Eu, G-EuP, G-Tb and G-TbP) was evaluated using the

3-(4,5-demithylthiazol-2-yl)-2,5-diphenyltetrazolium bromide (MTT) assay. Cells were treated with a serum-free medium containing Piroxicam, G-Eu, G-EuP, G-Tb or G-TbP at concentrations ranging from of 12.5, 25, 50, 100 and 200 μM of the piroxicam for 24 h. Then, the cells were incubated with 20 μl of 5 mg mL^{-1} MTT (Sigma-Aldrich, St. Louis, USA) dissolved in DMEM medium for 4 h. After this period, the supernatant was removed and dimethyl sulfoxide solution (150 μL $well^{-1}$) was added to each culture plate. After 15 min at room temperature, the absorbance was measured at 540 nm wavelength in a plate reader (TP-Reader, Thermoplate, Brazil). Relative cell viability, expressed as the percentage of the untreated cell (control, 100% viability), was calculated for each concentration. All data points represent an average of three independent assays.

Animal experiments: Female Swiss mice weighing 20–25 g were obtained from the breeding colonies of the Federal University of Alagoas (UFAL). Animals were maintained with free access to food and water and were kept at 22 ± 2°C with a controlled 12 h light-dark cycle at the Institute of Biological Science and Health animal housing facility. Experiments were performed during the light phase of the cycle. The animals were allowed to adapt to the laboratory for at least 4 h before testing and were used only once. Experiments were conducted under University Guidelines from the Committee for Animal Care and Use of Laboratory Animals (License no. 14512/2011-65).

Carrageenan-induced paw edema test in mice**:** Mice received a subplanter injection of 50 μL of carrageenan (300 μg/paw) in the right hind paw. The contra lateral paw received an injection of saline (NaCl, 0.9%). The volume of the paw was measured by a plethysmometer (Panlab, Spain) 4 h after the carrageenan injection. Edema was expressed as the difference in volume between the carrageenan-injected and the saline-injected paws [Δ paw volume (μL)].

Data were presented as the mean ± standard error of mean (S.E.M.) (n = 5). ANOVA followed by the Student–Neuman–Keuls test was used to compare the groups. A $P < 0.05$ was considered significant. All statistical analyses were performed using Graph Pad Prism 5.0 (Graph Pad Prism Software Inc., San Diego, CA, USA).

ESD setups: The distance between the cover glass and the capillary tip was 4 cm. The spray voltage applied varied between 26 and 30 kV and the injection rate was 1.7 mL h^{-1}. The solution was stored in a glass syringe connected to the capillary tip and the parameters adjusted. The sample was atomized into droplets by the applied high electrical potential. Then, the evaporation of solvent led to the formation of small hydrogel particles that were deposited in a glass substrate fixed above the capillary tip used to eject the solution.

Instruments: The Fourier-Transform IR spectra were acquired at room temperature using conventional KBr technique, in a range of 400 to 4000 cm^{-1}, with resolution of 4 cm^{-1}, on a Bruker IFS66 model. The thermogravimetric analysis was obtained in a TGA Shimadzu, model TGA-60 / 60H, using synthetic air and heating rate of 5°C / min. The x-ray diffraction patterns were obtained using a Bruker D8 Advanced diffractometer at ambient temperature in a 2θ range of 5º to 50º with increments of 0.02º, a velocity of 5º/min and an acquisition time of 1 sec. The photoluminescence measurements were obtained using a spectrofluorimeter Fluorog-3 ISA/Jobin-Yvon employing an excitation/emission slit of 3/2 mm and equipped with double excitation: 450 W Xe arc lamp and photomultiplier R928P. The Scanning Electron Microscopy (SEM) images were obtained by an FEI Quanta 200 3D model, under high vacuum and 20 keV. The transmission electron microscopic FEI Morgagni M268 model, with 100 kV acceleration, equipped with a Gatan Orius CCD. The rheological measurements were acquired using an Anton Paar MCR 101 rheometer. All CIE coordinates were obtained with Spectralux software®.[4]

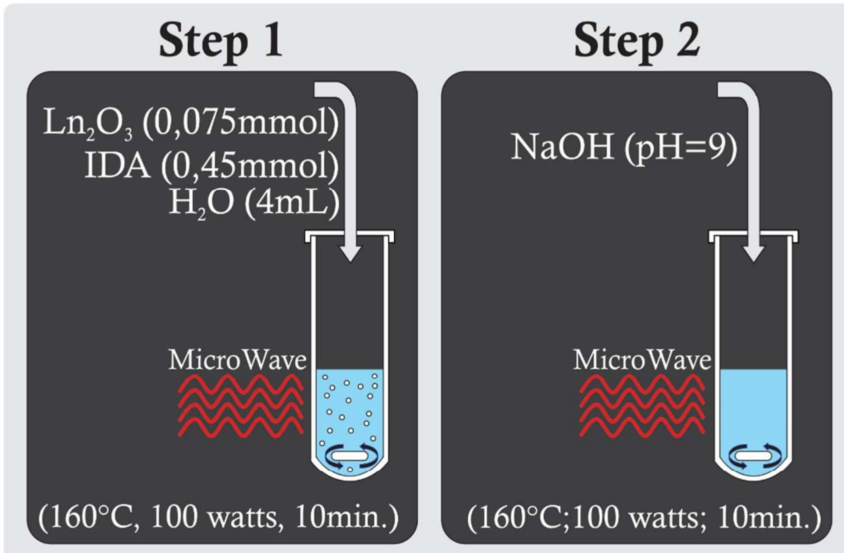

Scheme S1. Schematic two-steps method for hydrogel synthesis assisted by microwave.

Figure S1. Synthetized transparent hydrogel in an inverted cuvette.

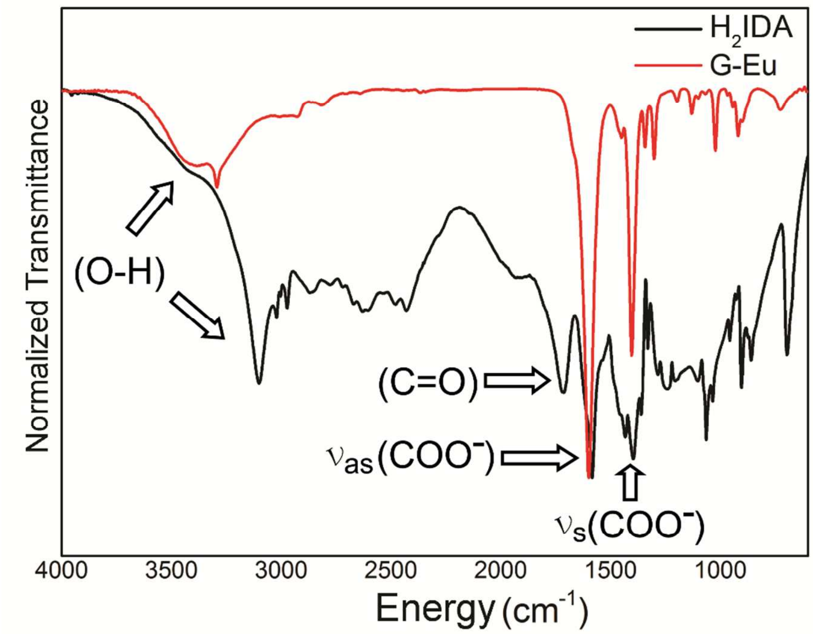

Figure S2. Fourier Transform IR spectra of as-prepared hydrogel Eu sample (G-Eu) and the pure ligand iminodiacetic acid (H_2IDA). The carboxyl group bands appear at 1594 cm^{-1} (asymmetric stretch) and 1413 cm^{-1} (symmetric stretch). These signals are displaced compared to the corresponding peak in pure ligand, which indicates a coordination bond with Eu^{3+}.

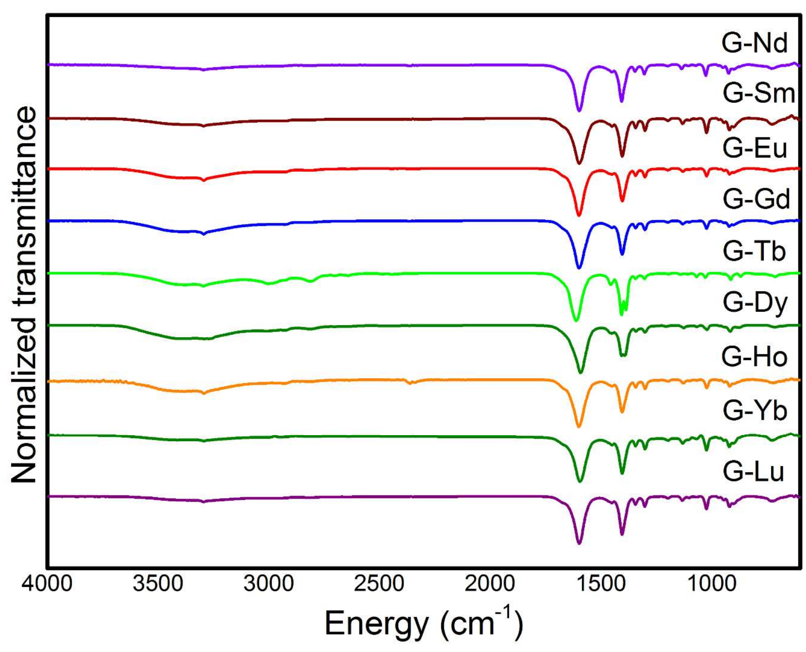

Figure S3. Fourier Transform IR spectra of all as-prepared hydrogels fabricated from lanthanide ions (Nd, Sm, Eu, Gd, Tb, Dy, Ho, Yb and Lu).

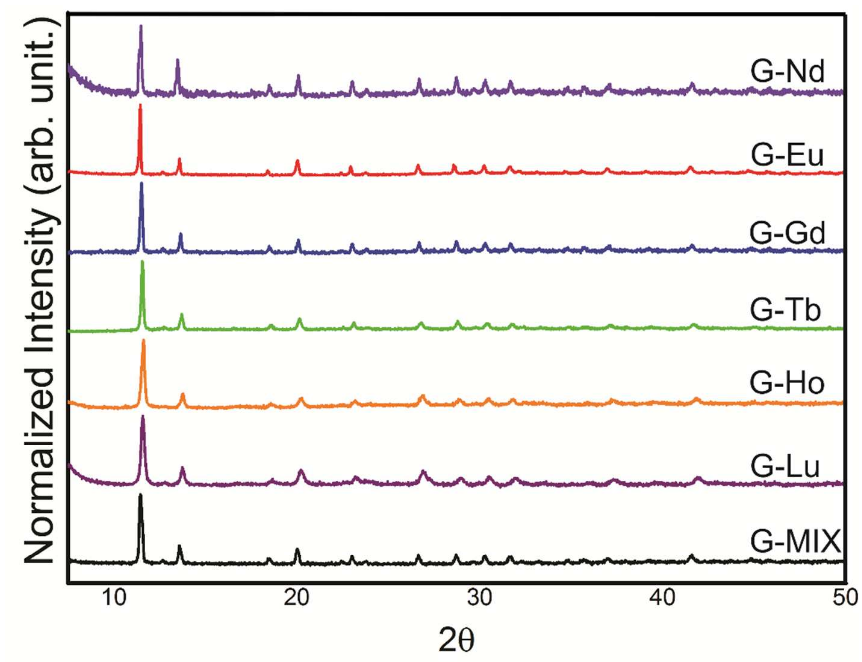

Figure S4. XRD patterns of as-prepared hydrogels with different lanthanide metals (Nd, Eu, Gd, Tb, Ho and Lu). Additionally, the XRD pattern of the probe sample based on the G-EuTb is presented as a G-mix.

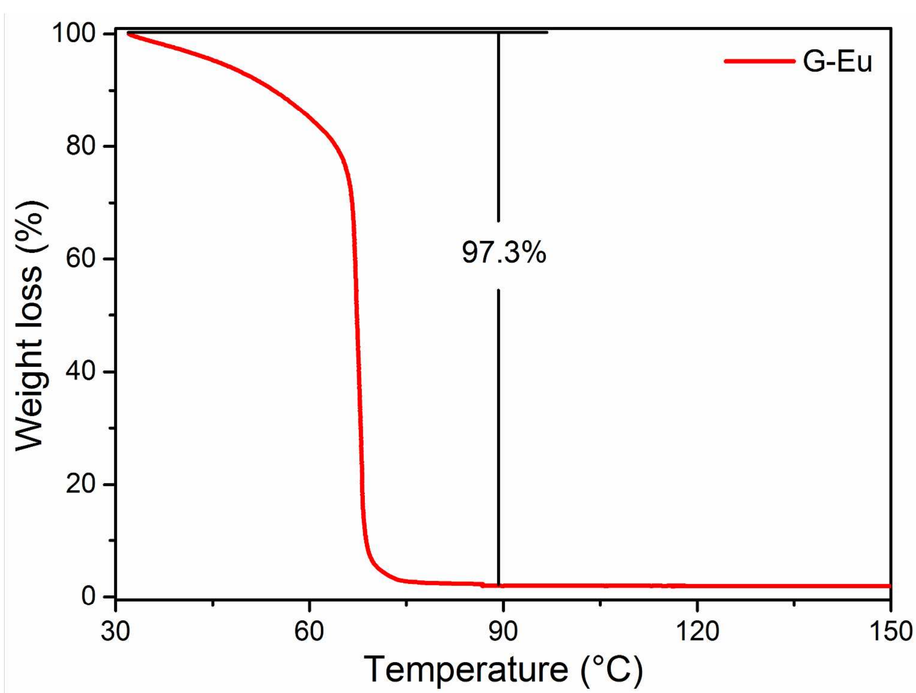

Figure S5. TGA curve of G-Eu.

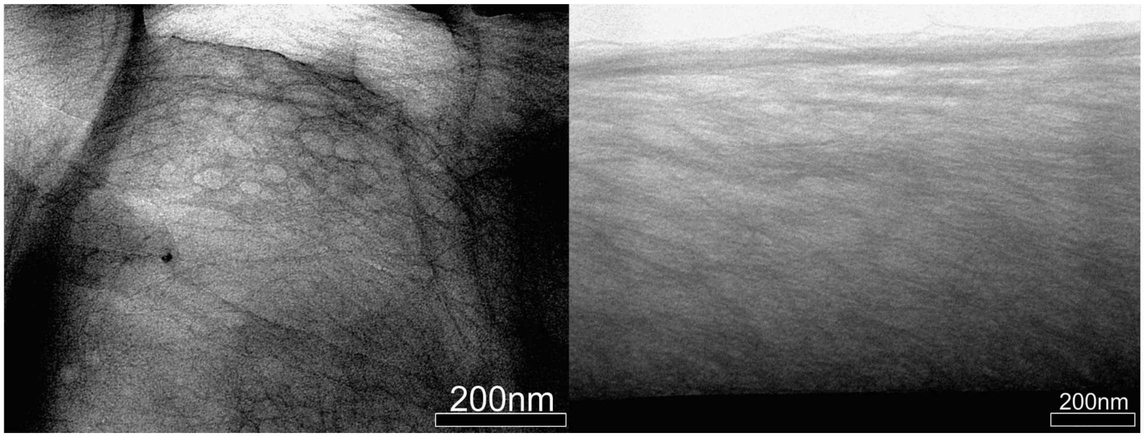

Figure S6. TEM micrographs of dry G-Eu.

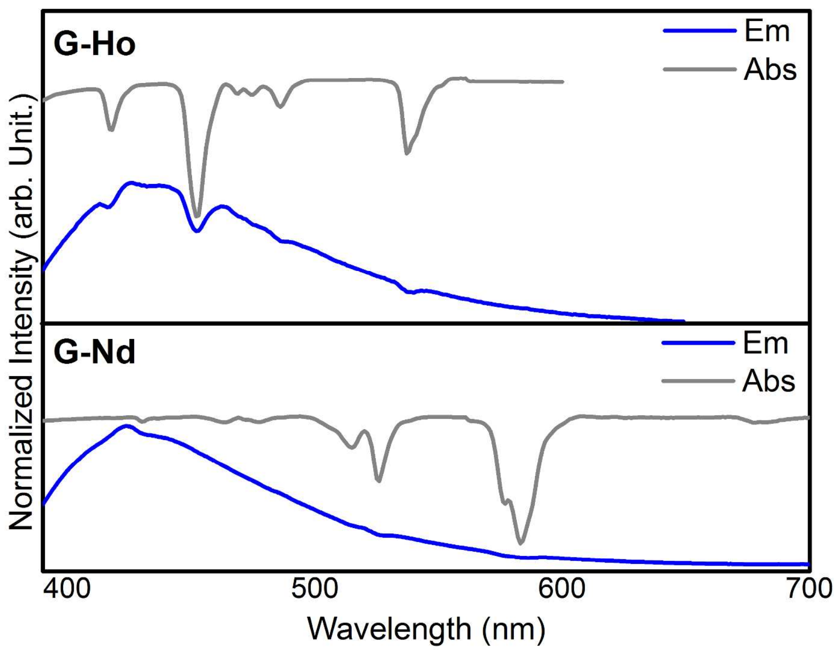

Figure S7. Emission and absorption spectrum of the G-Ho (above) and G-Nd (below) showing interferences from the effect of self-absorption. The emission spectrum (blue line) was acquired with excitation at 370 nm. The intensity data of absorption (grey line) was multiplied by (-1).

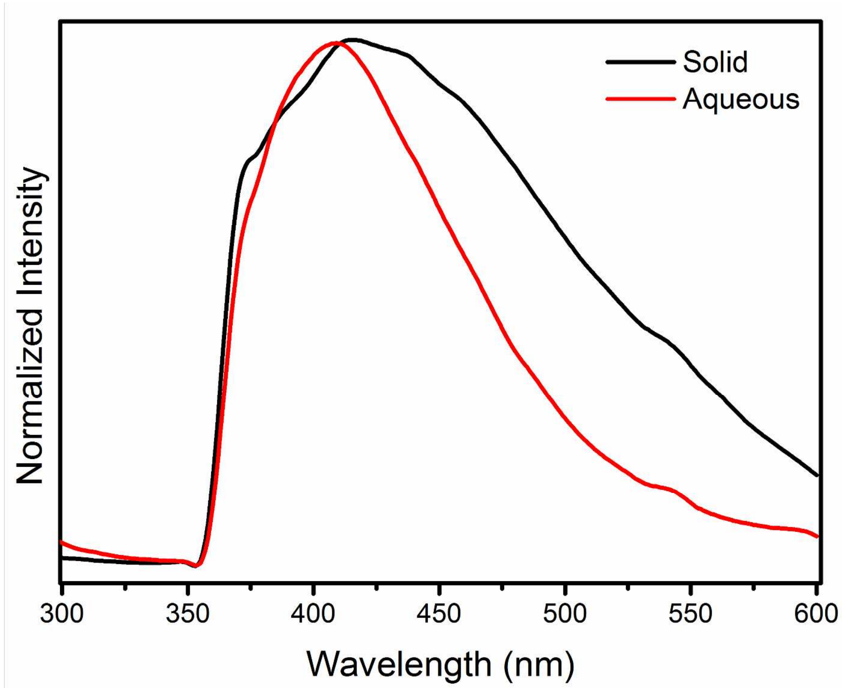

Figure S8. Emission spectra of H_2IDA in solid state (black line) and aqueous solution (red line).

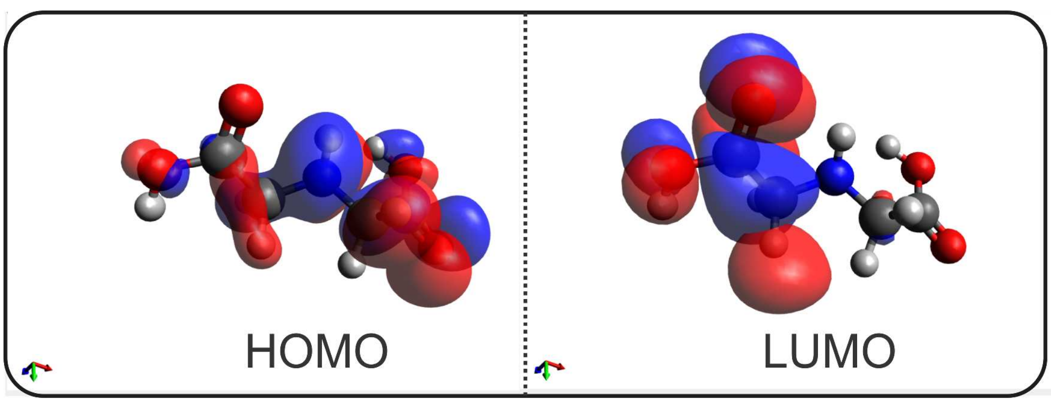

Figure S9. Spatial distribution of HOMO and LUMO density of iminodiacetic acid (H_2IDA) calculated using optimized geometries.

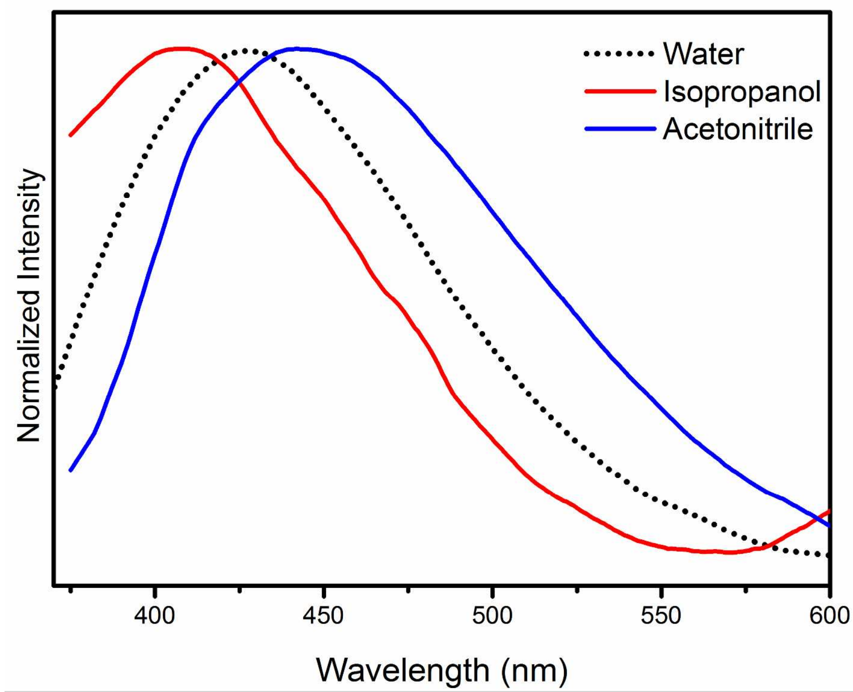

Figure S10. Emission spectrum of G-Lu in Water, Isopropanol, Acetonitrile.

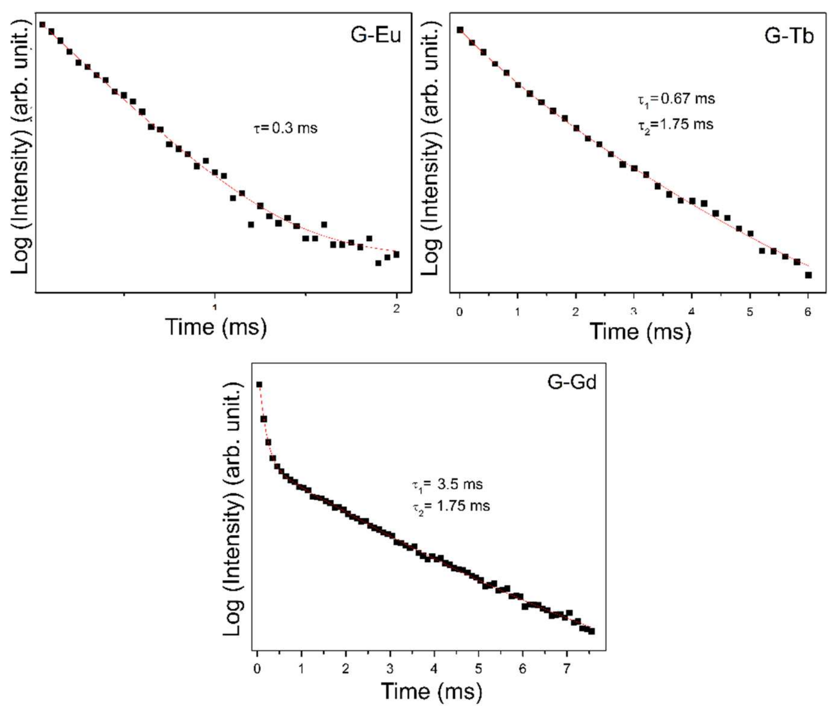

Figure S11. Decay curves and lifetimes of G-Eu (λ_{Ex}= 395 nm and λ_{Em}= 615 nm), G-Tb (λ_{Ex}= 370 nm and λ_{Em}= 544 nm) and G-Gd (λ_{Ex}=274 nm and λ_{Em}= 311 nm).

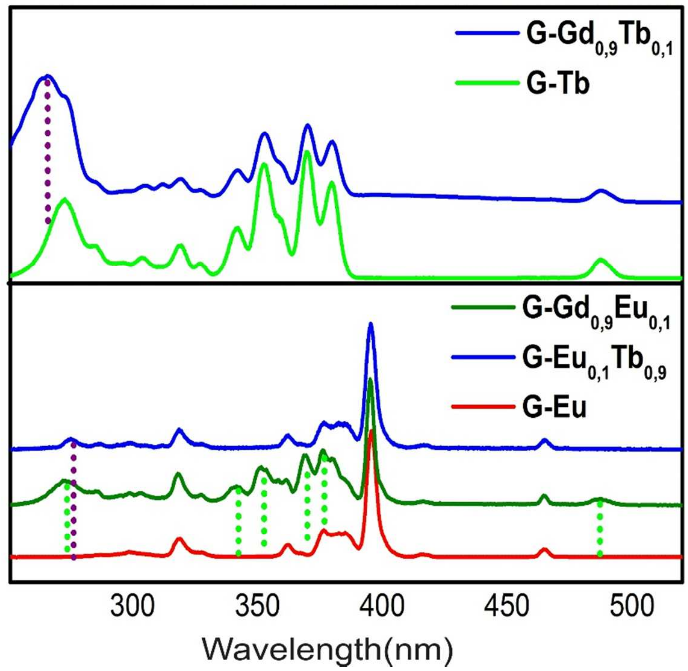

Figure S12. Excitation spectra for G-$Gd_{0.9}Tb_{0.1}$ (λ_{em}=544 nm, λ_{ex}=370 nm), G-Tb (λ_{em}=544 nm, λ_{ex}=370 nm), G-$Gd_{0.9}Eu_{0.1}$ (λ_{em}=615 nm, λ_{ex}=395 nm), G-$Eu_{0.1}Tb_{0.9}$ (λ_{em}=615 nm, λ_{ex}=370 nm) and G-Eu (λ_{em}=615 nm, λ_{ex}=395 nm).

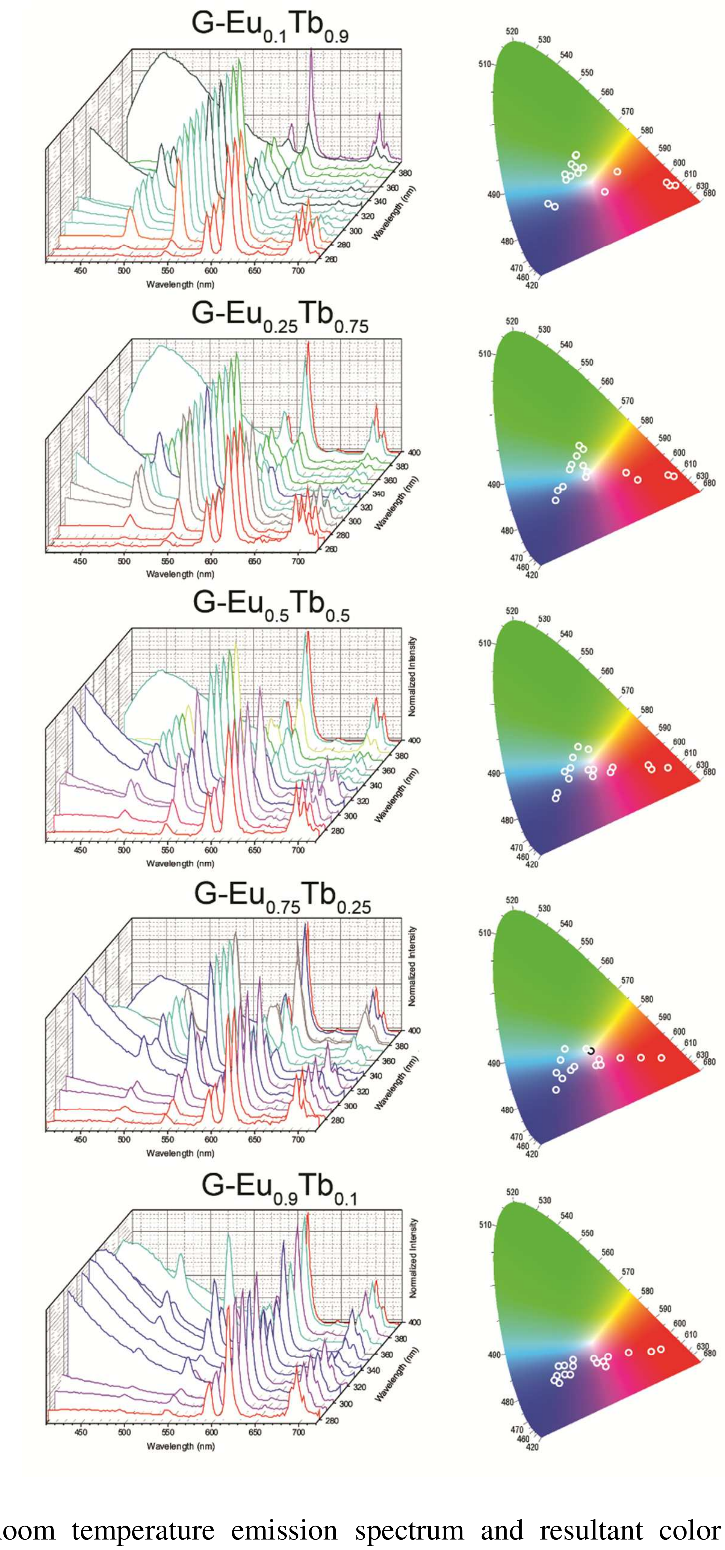

Figure S13. Room temperature emission spectrum and resultant color in CIE diagram, varying the excitation from 270 to 395 nm, of different dimetallic hydrogels G-Eu_xTb_x.

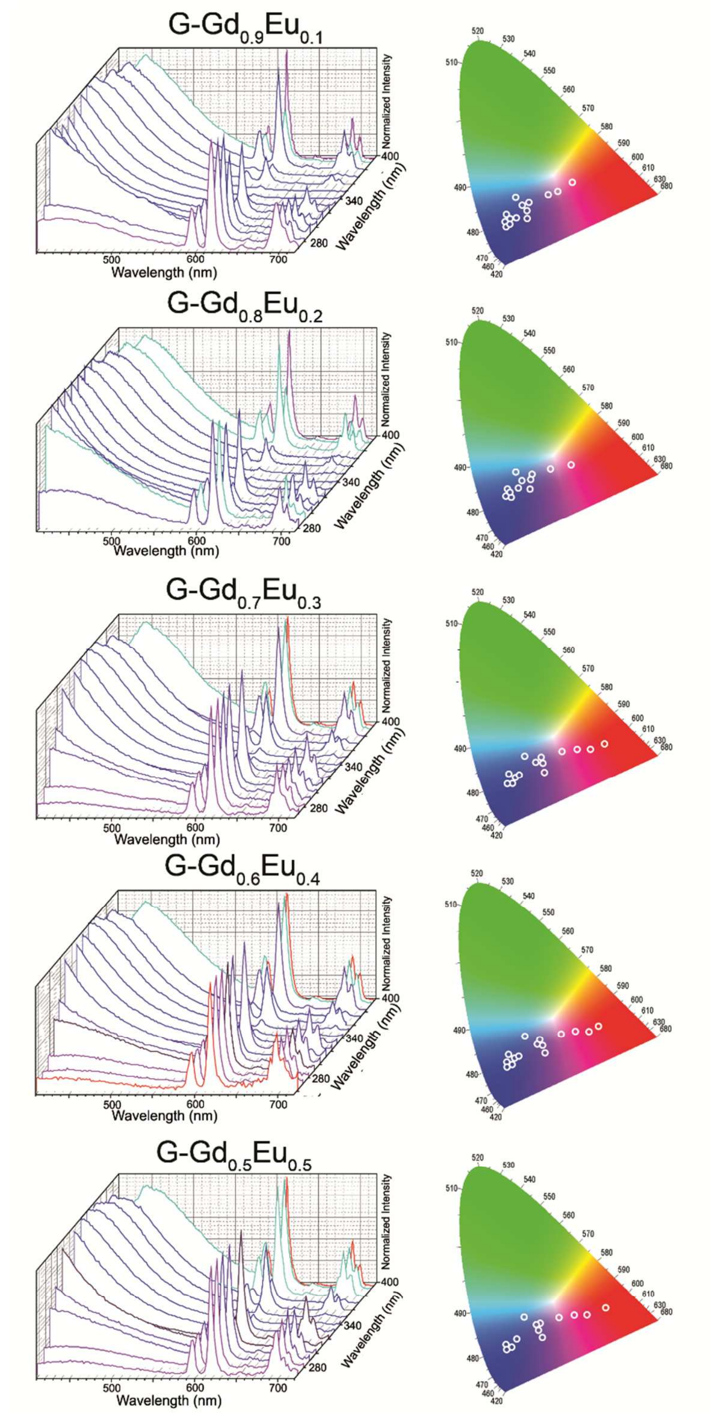

Figure S14. Room temperature emission spectrum and resultant color in CIE diagram, varying the excitation from 270 to 395 nm, of different dimetallic hydrogels G-$Gd_{1-x}Eu_x$.

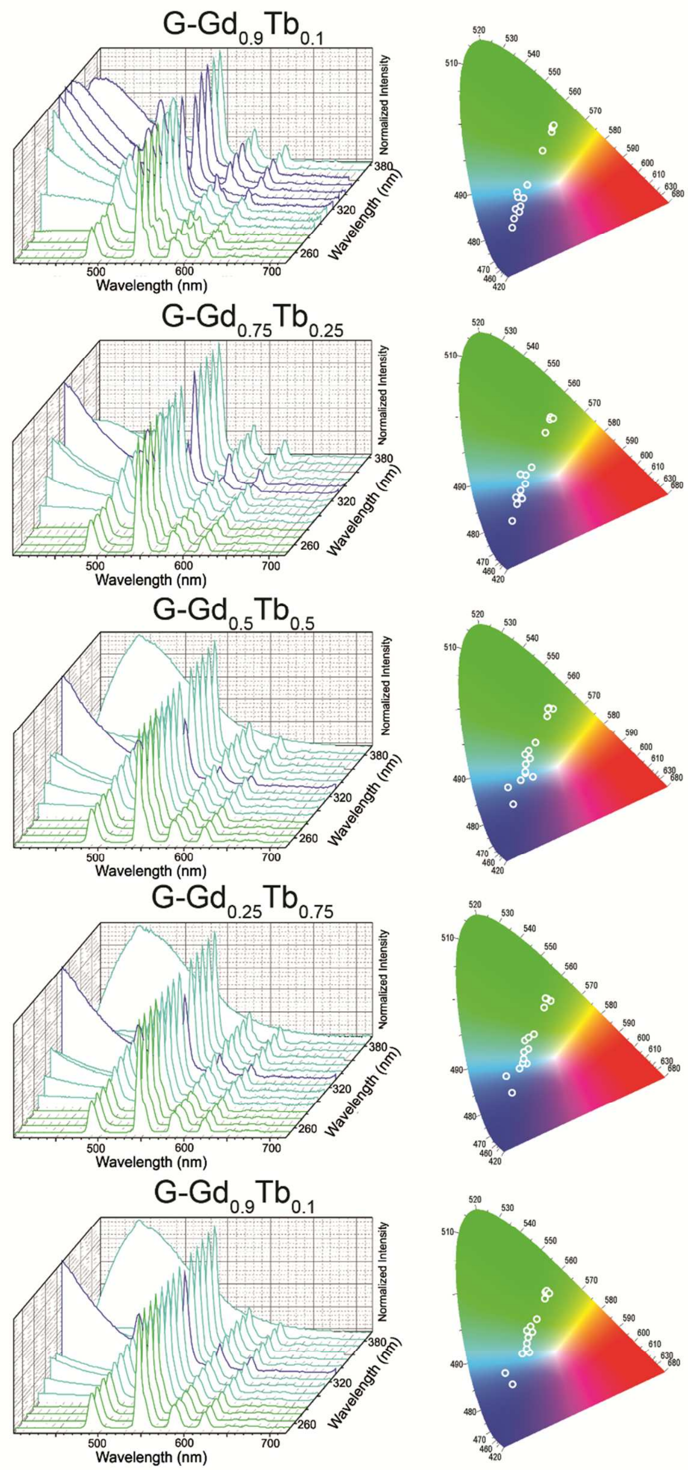

Figure S15. Room temperature emission spectrum and resultant color in CIE diagram, varying the excitation from 270 to 395 nm, of different dimetallic hydrogels G-$Gd_{1-x}Tb_x$.

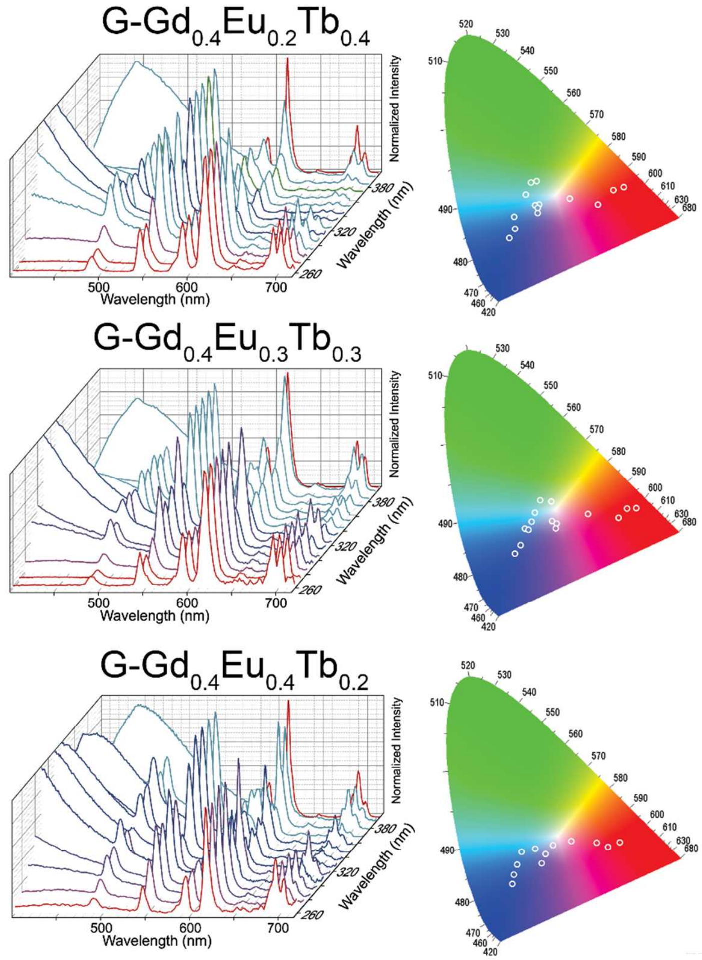

Figure S16. Room temperature emission spectrum and resultant color in CIE diagram, varying the excitation from 270 to 395 nm, of different trimetallic hydrogels $G\text{-}Gd_{0.4}Eu_{0.6\text{-}x}Tb_x$.

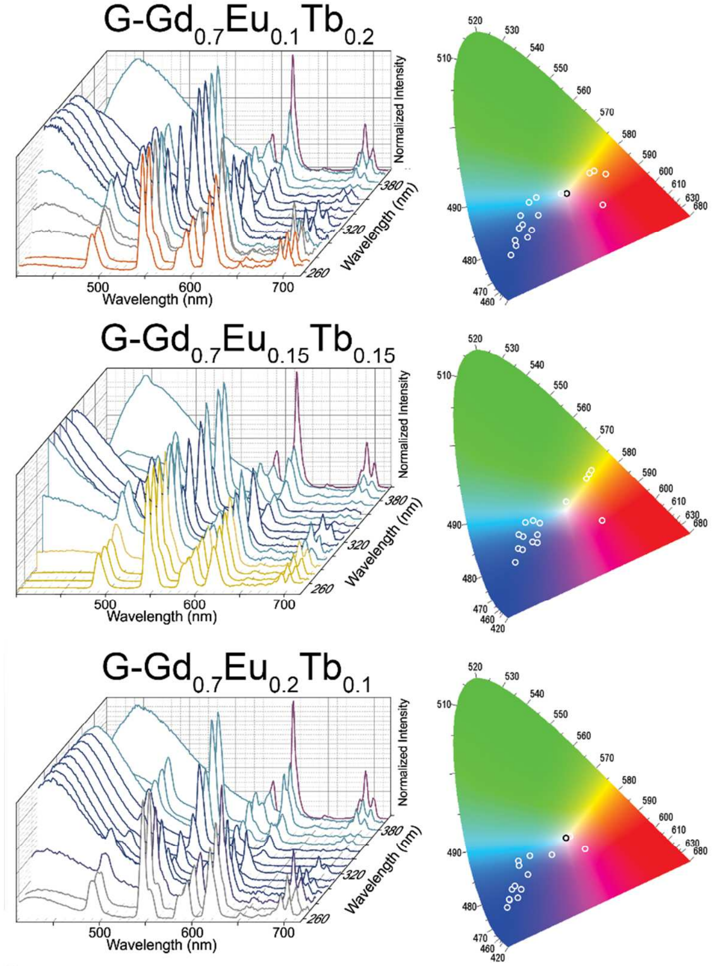

Figure S17. Room temperature emission spectrum and resultant color in CIE diagram, varying the excitation from 270 to 395 nm, of different trimetallic hydrogels G-$Gd_{0.7}Eu_{0.3\text{-}x}Tb_x$.

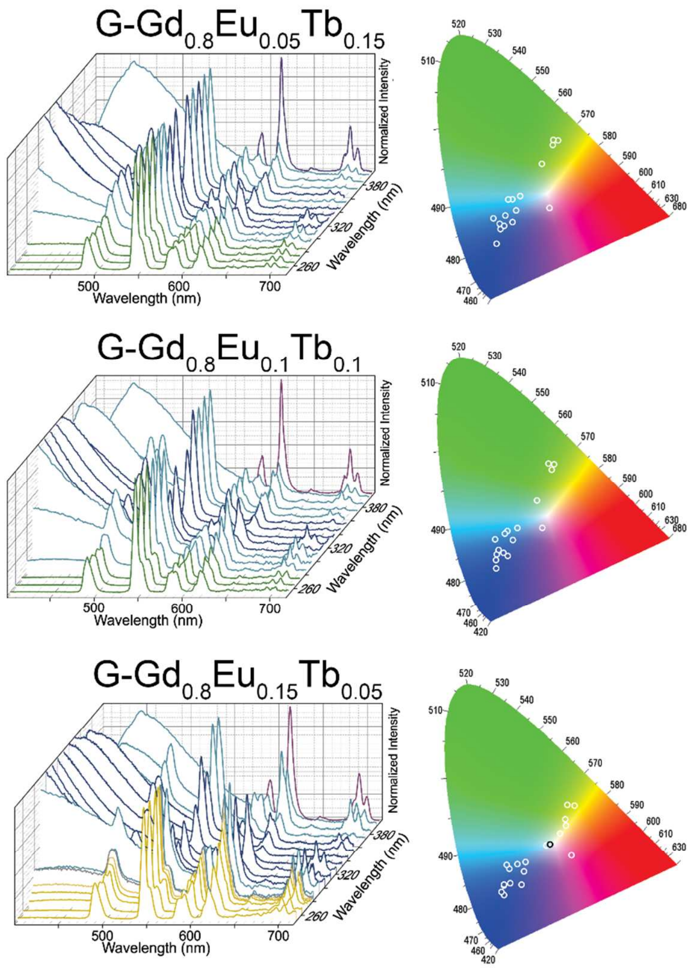

Figure S18. Room temperature emission spectrum and resultant color in CIE diagram, varying the excitation from 270 to 395 nm, of different trimetallic hydrogels G-$Gd_{0.8}Eu_{0.2-x}Tb_x$.

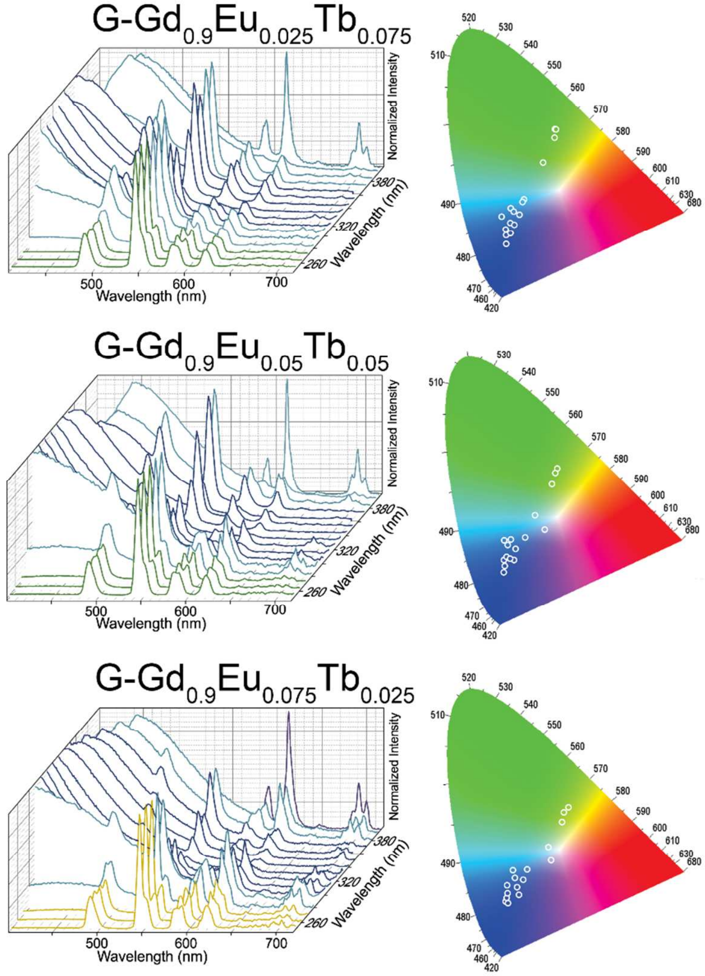

Figure S19. Room temperature emission spectrum and resultant color in CIE diagram, varying the excitation from 270 to 395 nm, of different trimetallic hydrogels G-$Gd_{0.9}Eu_{0.1-x}Tb_x$.

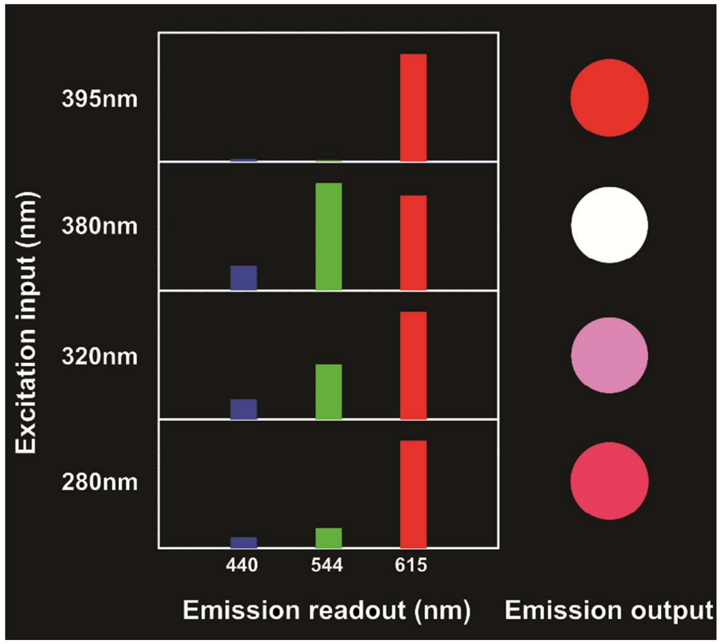

Figure S20. Two types of color-coded schematic barcode readout fashions integrating both visible and invisible information of the respective points of G-$Eu_{0.75}Tb_{0.25}$.

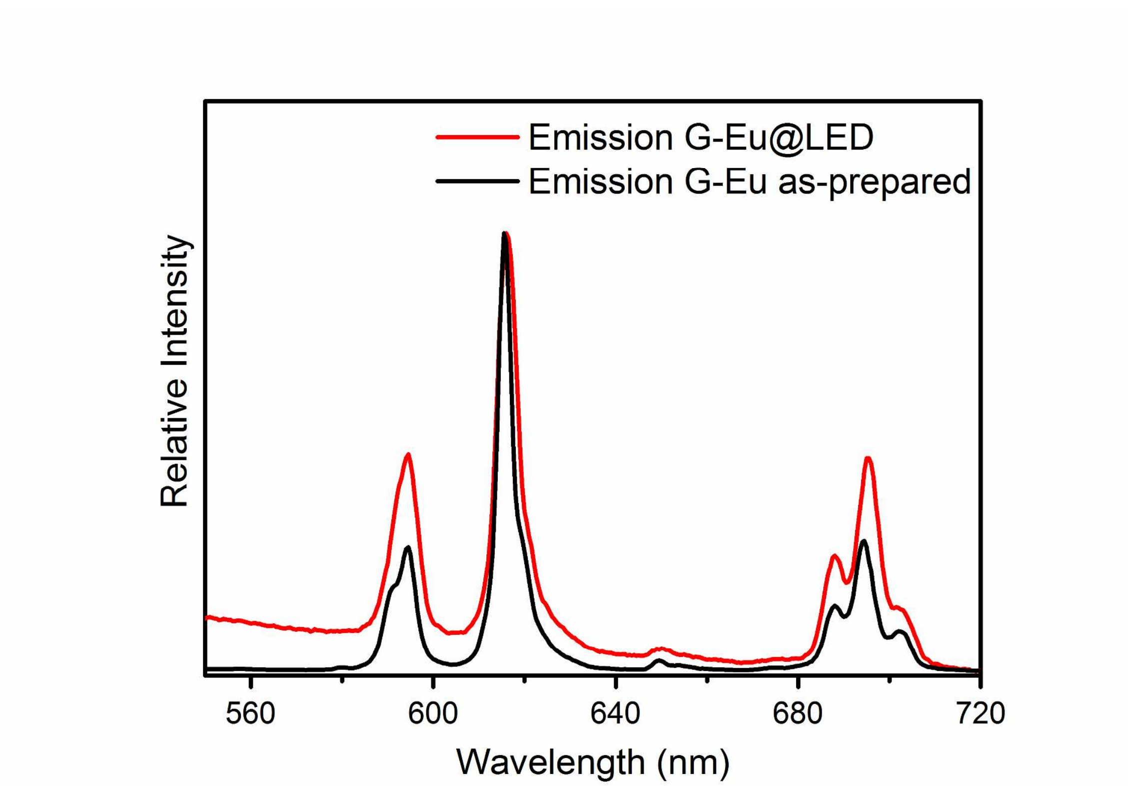

Figure S21. Room temperature emission spectrum of coated LED (G-Eu@LED) and as-prepared G-Eu.

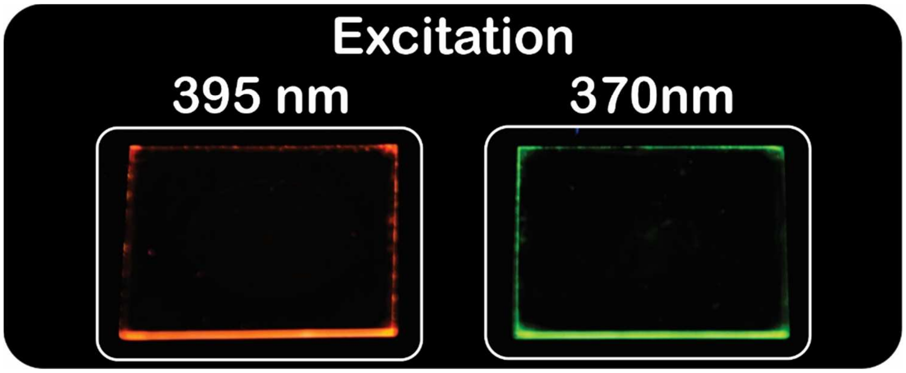

Figure S22. Thin-films coated by ESD onto glass.

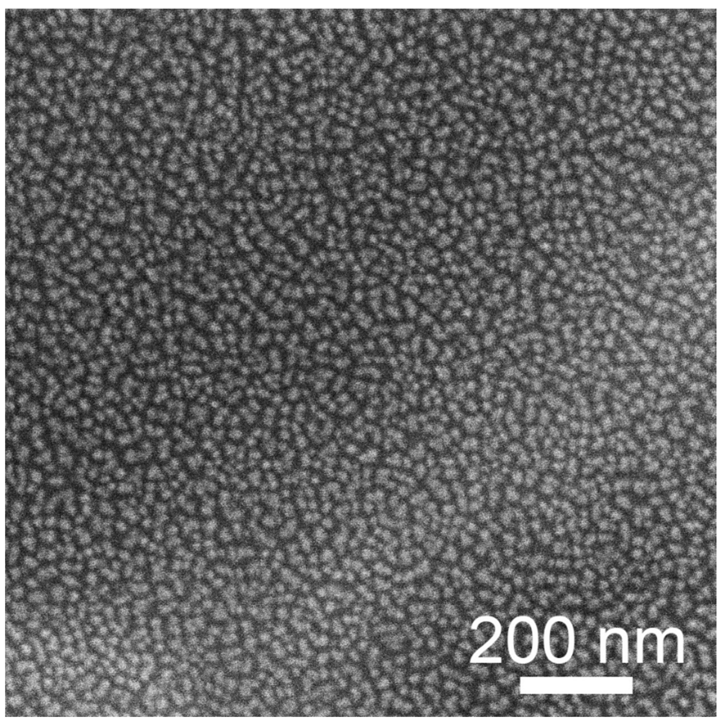

Figure S23. SEM images from the surface of G-Ln films obtained by the ESD method.

Figure S24. Envelope sealed with adhesive coated with G-Tb used in an infringement test.

Table S1. Photoluminescent information G-Ln.

G-Ln	λEx(nm)	Observed transitions	CIE (x,y)
G-Nd	581	$^4F_{3/2}\rightarrow{}^4I_J$ (J= 11/2 and 13/2)	0.17, 0.17
G-Sm	404	$^4G_{5/2}\rightarrow{}^6H_J$ (J=5/2, 7/2, 9/2, 11/2)	0.30, 0.32
G-Eu	395	$^5D_0\rightarrow{}^7F_J$ (J=0,1,2,3,4)	0.67, 0.32
G-Gd	274	$^6P_{3/2}\rightarrow{}^8S_J$ (J=3/2, 5/2, 7/2)	0.17, 0.17
G-Tb	370	$^5D_4\rightarrow{}^7F_J$ (J=6,5,4,3,2,1,0)	0.31, 0.54
G-Dy	365	$^4F_{9/2}\rightarrow{}^6H_J$ (J=15/2, 13/2, 11/2)	0.21, 0.29
G-Ho	471	$^5F_5\rightarrow{}^5I_7$	0.17, 0.20
G-Yb	370	$^2F_{5/2}\rightarrow{}^2F_{7/2}$	0.17, 0.14

Table S2. Lifetimes information.

LOGs	τ(ms)		
	Eu^{3+} (λ_{Ex}= 395 nm and λ_{Em}= 615 nm)	**Tb^{3+}** (λ_{Ex}= 370 nm and λ_{Em}= 544 nm)	
	τ	τ_1	τ_2
G-$Gd_{0,50}Eu_{0,50}$	0,30		
G-$Gd_{0,60}Eu_{0,40}$	0,30		
G-$Gd_{0,70}Eu_{0,30}$	0,30		
G-$Gd_{0,80}Eu_{0,20}$	0,33		
G-$Gd_{0,90}Eu_{0,10}$	0,32		
G-$Gd_{0,50}Tb_{0,50}$		0,30148	1,57188
G-$Gd_{0,60}Tb_{0,40}$		0,1594	1,6695
G-$Gd_{0,70}Tb_{0,30}$		0,78449	1,75395
G-$Gd_{0,80}Tb_{0,20}$		0,76776	2,11371
G-$Gd_{0,90}Tb_{0,10}$		0,98109	2,83202
G-$Eu_{0,10}Tb_{0,90}$	0,31	0,14684	1,447
G-$Eu_{0,25}Tb_{0,75}$	0,31	0,59784	1,8125
G-$Eu_{0,50}Tb_{0,50}$	0,26	0,2128	1,85324
G-$Eu_{0,75}Tb_{0,25}$	0,28	0,29224	1,67568
G-$Eu_{0,90}Tb_{0,10}$	0,25	0,11457	0,5704
G-$Gd_{0,90}Eu_{0,025}Tb_{0,075}$	0,37	0,646	2,47467
G-$Gd_{0,90}Eu_{0,05}Tb_{0,05}$	0,34	0,612	2,64528
G-$Gd_{0,90}Eu_{0,075}Tb_{0,025}$	0,34	0,266	2,06109
G-$Gd_{0,80}Eu_{0,05}Tb_{0,15}$	0,31	0,205	1,6745
G-$Gd_{0,80}Eu_{0,10}Tb_{0,10}$	0,36	0,5239	2,37197
G-$Gd_{0,80}Eu_{0,15}Tb_{0,05}$	0,30	0,26681	1,80178
G-$Gd_{0,70}Eu_{0,10}Tb_{0,20}$	0,29	0,35164	1,799
G-$Gd_{0,70}Eu_{0,15}Tb_{0,15}$	0,30	0,527	1,77253
G-$Gd_{0,70}Eu_{0,20}Tb_{0,10}$	0,30	0,310	1,79092
G-$Gd_{0,40}Eu_{0,20}Tb_{0,40}$	0,31	0,283	1,9407
G-$Gd_{0,40}Eu_{0,30}Tb_{0,30}$	0,29	0,209	1,84714
G-$Gd_{0,40}Eu_{0,40}Tb_{0,20}$	0,25	0,046	0,68443

REFERENCES

(1) da Silva, F. F.; de Menezes, F. L.; da Luz, L. L.; Alves, S. Supramolecular Luminescent Hydrogels Based on [Small Beta]-Amino Acid and Lanthanide Ions Obtained by Self-Assembled Hydrothermal Reactions. *New J. Chem.* **2014**, *38* (3), 893–896.

(2) Schmidt, M. W.; Baldridge, K. K.; Boatz, J. A.; Elbert, S. T.; Gordon, M. S.; Jensen, J. H.; Koseki, S.; Matsunaga, N.; Nguyen, K. A.; Su, S. General Atomic and Molecular Electronic Structure System. *J. Comput. Chem.* **1993**, *14* (11), 1347–1363.

(3) Hanwell, M. D.; Curtis, D. E.; Lonie, D. C.; Vandermeersch, T.; Zurek, E.; Hutchison, G. R. Avogadro: An Advanced Semantic Chemical Editor, Visualization, and Analysis Platform. *J. Cheminformatics* **2012**, *4* (1), 17.

(4) Santa-Cruz, P. A.; Teles, F. S. Spectra Lux Software v. 2.0, Ponto Quântico Nanodispositivos. *Spectra Lux Softw. v. 2.0; Ponto Quântico Nanodispositivos* **2003**.